CHAPTER II

Review of high energy interaction models

1. Introduction :

At accelerator energies (centre of mass energy, $\sqrt{s}$) up to 1.8 TeV the most remarkable fact about high energy hadron-hadron collision is the continuous rise in total cross section (σ_T) consistent with $\log^2 s$ (Rubinstein ,1990; Demarteau ,1992). Intense experimental studies and theoretical efforts have been made for a better understanding of the process of multiparticle production at high energy (Fermi ,1950, 1951; Landau ,1956; Cocconi ,1958; Feynman ,1969; Benecke et al.,1969; Koba et al.,1972; Gaisser & Yodh,1980; Zalewski ,1985). Various kinematic parameters, like total cross section (σ_T), charged particle multiplicity (n), transverse momentum (p_t) etc., have been studied precisely by accelerators at CERN and FNAL up to an energy of about 2 TeV in the last three decades (Bertin et al.,1972; Slattery ,1973; Dao et al.,1973; Capiluppi et al.,1974; Clark et al.,1978; Banner et al.,1982; Alner et al.,1984,1985). At energies higher than that attained by the accelerators the interaction characteristics are studied by cosmic ray experiments extrapolating the behaviour of the kinematic parameters from accelerator energy range to cosmic ray primary particle energy through various interaction models. In this chapter a brief discussion on high energy interaction models is given. Some basic terminologies regarding those interaction models are explained before entering into model discussion.

Centre of mass (CM) energy :

Studies on high energy interactions in the laboratory become feasible due to two types of accelerators :

(i) fixed target accelerators in which the projectile beam interacts with stationary nucleons and (ii) colliding beam accelerators in which two beams of particles of equal but opposite momentum interact.

In either type of accelerator the energy available for the production of particles is the CM energy. For the interaction of particle 'a' of mass m_a and laboratory (L) energy W_a with particle 'b' of mass m_b, the CM energy squared is given by,

$$s = m_a^2 + m_b^2 + 2m_bW_a \qquad \ldots(2.1)$$

Approximately,

$$s \simeq 2m_bW_a, \qquad \ldots(2.2)$$

when s large compared to m_a^2 and m_b^2.

Thus in case of fixed target accelerator experiments the CM energy, $\sqrt{s}$ is proportional to the square root of the projectile energy in the L-system (W_a).

But in case of colliding beam accelerators, in which the beam energies are W_a and W_b, the quantity s becomes,

$$s = (W_a + W_b)^2 \qquad \ldots(2.3)$$

Thus in colliding beam accelerators large CM energy can be achieved as

$$\sqrt{s} \propto W, \qquad \ldots(2.4)$$

when $W_a = W_b = W$.

Multiplicity :

The number of charged particles coming out of an inelastic interaction is called the charged particle multiplicity (n). As energy increases, both the spread in 'n' and the average $\langle n \rangle$ increases because more energy is available for conversion

into mass. The best fit to the experimental data suggests the relationship between multiplicity and energy as,

$$n = A + B\ln s + Cs^{q}, \qquad \ldots(2.5)$$

where A, B, C and q are constants.

In high energy collisions the most of the produced hadrons are pions. At the same energy ($\sqrt{s}$) if we sum over all inelastic channels the average multiplicities of three charged states of pions are found experimentally to be

$$\langle n_{\pi^+} \rangle \simeq \langle n_{\pi^-} \rangle \simeq \langle n_{\pi^0} \rangle.$$

Inelasticity :

The fraction of incident energy carried away by the secondary particles produced is called the inelasticity (K_s) of the interaction at that energy,

$$K_s = \sum_i \langle n_i \rangle \langle E_i \rangle / W, \qquad \ldots(2.6)$$

where W is the incident energy and $\langle n_i \rangle$, $\langle E_i \rangle$ are average multiplicity and average energy of each kind of secondary. The summation is over all kinds of secondary particles.

In inelastic interactions the sum of the fraction of energy taken by the leading particle (K_l) and the quantity K_s should be equal to unity, i.e.,

$$K_s + K_l = 1. \qquad \ldots(2.7)$$

Inclusive reactions :

Inclusive reactions are those in which we look for a specific particle out of all possible final particle states. In an inclusive reaction of the type,

$$a + b = c + \text{anything}$$

only the secondary particle 'c' is registered. This type of reaction is called one-particle inclusive reaction.

2. Fermi's statistical model and thermodynamic model :

According to statistical model (Fermi ,1950,1951) when two nucleons collide with very high energy in their CM system this energy is suddenly released in a small volume surrounding the two nucleons. This volume is occupied by the two nucleons surrounded by pion field. The volume (v) is fixed by the range of strong interactions, $v \sim (\hbar/m_\pi c)^3$, where m_π is the pion mass. The energy concentrated within this volume is distributed among the various degrees of freedom according to statistical laws. It is assumed that the concentrated energy is then converted into hadrons which are emitted in all directions.

According to this model the average multiplicity $\langle n \rangle \propto s^{1/3}$, which does not reflect the experimental facts. It also conflicts with the anisotropy of particle momentum distribution in CM system.

Thermodynamic model is a modified version of statistical model. One thinks a gas of pions confined in the volume, $v \sim (\hbar/m_\pi c)^3$ with total CM energy $\sqrt{s}$ at temperature T. For simplicity one assumes that the final state consists only of π^+, π^0 and π^- and that the statistical weights of each of these charged states are equal.

The most probable number of pions per unit energy interval per unit volume at temperature T is,

$$dN(E)/dE = (3E^2/2\pi^2c^3\hbar^3)\,[\exp(E/kT)-1]^{-1}, \quad \ldots(2.8)$$

where E is the energy of the pion and k is the Boltzmann constant.

From usual thermodynamic concepts, integrating equation (2.8) for $0 \leqslant E \leqslant \infty$ and using natural units $\hbar=c=1$ we

get the average total number of pions per unit volume,

$$\langle N \rangle = \emptyset.36(kT)^3. \qquad \ldots(2.9)$$

The total energy per unit volume is,

$$u = \int_0^\infty (3E^3/2\Pi^2)\,[\exp(E/kT)-1]^{-1}dE \simeq (kT)^4 \qquad \ldots(2.1\emptyset)$$

Also,

$$u = \sqrt{s}/v \qquad \ldots(2.11)$$

From equations (2.1Ø) and (2.11), we get

$$kT = (\sqrt{s}/v)^{1/4} \qquad \ldots(2.12)$$

Therefore, from equation (2.9),

$$\langle N \rangle = \emptyset.36(\sqrt{s}/v)^{3/4} \qquad \ldots(2.13)$$

Considering v to be independent of energy, the average multiplicity,

$$\langle n \rangle = \langle N \rangle v = \text{constant}.(s)^{3/8} \qquad \ldots(2.14)$$

This result is in crude agreement with experiments.

3. The hydrodynamic model :

Landau (1956) suggested that the colliding particles release the whole of the energy in a compound system of small volume in which large number of strongly interacting particles are formed with interaction mean free path small compared to the dimension of the system and a statistical equilibrium is set up. The compound system then expands like an ideal, non-viscous fluid with zero thermal conductivity. During the hydrodynamic state of expansion the number of particles inside the volume is not constant because the strongly interacting particles inside the small volume constantly produced and absorbed in the compound system. Expansion process continues until the mean free path of the interacting particles become comparable to the linear dimension of the compound system when

the interaction between the particles becomes weaker. The emission of secondaries (hadrons) occur when the compound system breaks up at the end of expansion. Landau calculated that in hydrodynamic model the total multiplicity,

$$n \simeq W^{1/4}, \qquad \ldots(2.15)$$

where W is the energy in the laboratory system.

4. The fireball model :

The fireball model (Cocconi ,1958) assumes that the two incident hadrons interact through a forward dominant process in the CM frame. The forward dominant process indicates that in the CM frame the differential cross sections or angular distributions are dominated by particles going forward along the direction of motion of both the interacting incident particles. It also says that transverse momenta are relatively small. The incident hadrons are then exited to higher unstable states [starred('*') states] called the 'fireballs'. Fireballs are thought of as lumps of purely mesonic matter.

The decay of each fireball is independent of the other and is also independent of how the fireballs are produced. Each fireball decays isotropically in its own rest frame. After the decay of the fireballs at least two of these particles carry the baryon number and strangeness of the incident particles. For the fireball of mass M_i^* (in excited state) the decay is represented by,

$$M_i^* \text{ ----> particle } i + n_i \text{ pions}$$

assuming that (i) in the M_i^* rest frame each pion has the same total energy E_π , (ii) the kinetic energy of the particle 'i' is

negligible if it is a nucleon and (iii) E_π is a constant independent of M_i^* and s (CM energy squared).

The number of pions produced by the decay of the fireball is,

$$n_i(M_i^*) = (M_i^* - M_i)/E_\pi , \qquad \ldots(2.16)$$

where M_i is the mass of the incident hadron.

5. Feynman scaling :

Feynman (1969) put forward the scaling hypothesis. Considering the CM frame of the one-particle inclusive reaction,

$$a + b = c + \text{anything}$$

the longitudinal and transverse momemtum of the particle 'c' are,

$$p_l = p \text{ Cos } \theta$$
$$p_t = p \text{ Sin } \theta \qquad \ldots(2.17)$$

respectively, where p and θ are CM momentum and production angle of particle 'c'.

The so called transverse mass

$$m_t = (E^2 - p_l^2)^{1/2} = (p_t^2 + m^2)^{1/2}, \qquad \ldots(2.18)$$

where $E=(p^2+m^2)^{1/2}$ is the energy of the secondary (c) and m is its mass.

The Feynman variable (x) is defined as

$$x = p_l/p_{lmax} \xrightarrow{s \to \infty} 2p_l/\sqrt{s}, \qquad \ldots(2.19)$$

where p_{lmax} is the maximum possible momentum that particle 'c' can have in the CM system and $\sqrt{s}$ is the CM energy.

Thus the range of x is,

$$-1 \leqslant x \leqslant +1,$$

where negetive x means particles with p_l negative.

Lorentz invariant phase space is given by,

$$dL_{ips} = d^3p/E \qquad \ldots(2.20)$$

The Lorentz invariant inclusive cross section is $d\sigma/dL_{ips}$ and is written as,

$$E(d^3\sigma/d^3p) = f(p,s). \qquad \ldots(2.21)$$

Although f is Lorentz invariant, the quantity p used to specify it is not Lorentz invariant.

In terms of p_t, p_l and ϕ the phase space is

$$d^3p/E = d\phi(dp_t^2/2)(dp_l/E), \qquad \ldots(2.22)$$

where ϕ is the azimuth angle, varies from Ø to 2π .

The invariant momentum distribution (2.21) then takes the form,

$$(E/\pi)(d^2\sigma/dp_t^2 dp_l) = f(p_t, p_l, s) \qquad \ldots(2.23)$$

p_t is the momentum component of the secondary 'c' transverse to the direction of motion of particles 'a' and 'b' and p_l is its momentum component along the direction, taken as positive when the particle 'c' is moving in the same direction as particle 'a'. p_t is invariant to Lorentz velocity transformations along the direction of motion of particles 'a' and 'b'; but p_l and E are not invariant under such transformations.

Since the p_t distribution has a sharp cut off as energy increases, the average value of p_l must increase. To cancel this effect the Feynman variable ($x=p_l/p_{lmax} \simeq 2p_l/\sqrt{s}$) is introduced and equation (2.23) takes the form

$$(2E/\pi\sqrt{s})(d^2\sigma/dp_t^2 dx) = f(p_t, x, s) \qquad \ldots(2.24)$$

According to Feynman scaling hypothesis, the inclusive cross section for a given type of secondary particle can be written as,

$$E(d^3\sigma/d^3p) = f(p_t,x,s) \xrightarrow[s\to\infty]{} f(x,p_t), \qquad \ldots(2.25)$$

which is called the scaling behaviour of the inclusive cross sections. The longitudinal momentum distribution of each type of secondary particles is independent of energy when measured (scaled) in terms of the incident momentum.

Another longitudinal variable of the secondary particle 'c' is called the CM rapidity (y) which is given by

$$y = \emptyset.5\ln\{(E+p_l)/(E-p_l)\} = \ln\{(E+p_l)/m_t\}. \quad ...(2.26)$$

The relation between the Feynman scaling variable (x) and the rapidity variable (y) is nonlinear:

$$x = (2/\sqrt{s})(p_t^2+m^2)^{1/2}\mathrm{Sinh}\ y. \quad ...(2.27)$$

The maximum longitudinal momentum a particle can attain in a collision in the CM system is half the CM energy. Thus the maximum rapidity value in the CM system is restricted to

$$y_{max} = \ln(2E/m_t) = \emptyset.5\ln(s/m_t^2). \quad ...(2.28)$$

In terms of rapidity equation (2.24) reduces to

$$d^2\sigma/\pi\, dp_t^2 dy = f(p_t, y, s). \quad ...(2.29)$$

In this case also, according to Feynman scaling hypothesis, the inclusive cross section for a given type of secondary tend to an incident energy independent limit as energy increases, i.e.,

$$E(d^3\sigma/d^3p) = f(p_t, y, s) \xrightarrow[s \to \infty]{} f(p_t, y). \quad ...(2.30)$$

In the high momentum limit when the masses of the particles can be neglected, the argument in the logarithm of the rapidity variable (y) can be directly related to the angle θ which the momentum of the secondary particle (c) makes with respect to the direction of incident particle 'a' then,

$$y = \emptyset.5\ln\{(E+p_l)/(E-p_l)\} \approx \emptyset.5\ln\{\mathrm{Cos}^2(\theta/2)/\mathrm{Sin}^2(\theta/2)\}$$

$$\text{i.e.,}\quad y = \ln\{\mathrm{Cot}(\theta/2)\} \equiv \eta \quad . \quad ...(2.31)$$

The angular variable $\eta = \ln\{\mathrm{Cot}(\theta/2)\}$ is called the pseudorapidity.

6. The fragmentation model :

A remarkable feature of multiparticle production process in high energy particle interaction is the small value of the transverse momenta (p_t) and the quite large value of the longitudinal momenta (p_l) of the secondary particles. Fragmentation model (Benecke et al.,1969) had been developed to accomodate these two dominant features of high energy interactions.

In the interaction process,

$$a + b \longrightarrow c + d + e + \ldots\ldots\ ,$$

in which 'a'(projectile) excites 'b'(target), and subsequent decay of 'b' gives the target fragmentation products c, d, e.....etc.

Physically the target behaves as an absorbing medium through which the projectile propagates. In such a picture, the projectile in the rest frame of the target (L-frame) contracts into a thin disk due to Lorentz contraction at high energies. The passage of this thin disk through the target (during small but finite time) causes excitation of the target and subsequent breakup of the target into fragments.

Let p_c is the momentum of the particle 'c' produced in the above interaction process. The fragmentation model says that the probability of producing the particle 'c' with momentum p_c is independent of s as $s \longrightarrow \infty$.

We consider the rest frame of any one of the colliding

particles (i.e., a or b). If a particle 'c' is produced in an interaction process with momentum p_c, then according to the uncertainty principle the linear dimension of the volume of interaction will be

$$L_c \sim \hbar/p_c. \qquad \ldots(2.32)$$

Due to Lorentz contraction at high energy, the projectile 'a' shrinks into a thin disk, the thickness (T_a) of which is given by

$$T_a \propto 1/\sqrt{s}. \qquad \ldots(2.33)$$

When $T_a << L_c$, i.e., $\sqrt{s} >> p_c$, the production of particle 'c' by fragmentation process with momentum p_c does not depend on s as $s \longrightarrow \infty$. For any p_c with respect to the target (b) frame $|p_c|/\sqrt{s} \longrightarrow \emptyset$ as $s \longrightarrow \infty$.

For any fixed p_c, the requirement $T_a << L_c$ is attained at sufficiently high energy. Thus the fragmentation model predicts that the distribution in p_c approaches a limit as $s \longrightarrow \infty$.

Explicitly, it may be written as, for the target (b) fragmentation,

$$f_b(p_t, p_l, s) \xrightarrow[s \longrightarrow \infty]{} f_b(p_t, p_l), \qquad \ldots(2.34)$$

in the rest frame of the target (b).

Similarly, for the particles produced due to projectile (a) fragmentation,

$$f_a(p_t, p_l, s) \xrightarrow[s \longrightarrow \infty]{} f_a(p_t, p_l), \qquad \ldots(2.35)$$

in the rest frame of the projectile (a).

Let p_{lc} be the longitudinal momentum of particle 'c' in the rest frame of the target (b), i.e., the L-frame. Then, as $s \longrightarrow \infty$,

$$p_{lc} = (x+|x|)(s/4m_b)+(p_t^2+m_c^2-x^2m_b)/2m_b|x|, \qquad \ldots(2.36)$$

where m_b, m_c are the masses of the particles 'b' and 'c'.

For $-1 \leqslant x < \emptyset$, as $s \dashrightarrow \infty$,

$$p_{lc} = (p_t^2 + m_c^2 - x^2 m_b)/2m_b|x| \qquad \ldots(2.37)$$

in the rest frame of the target (b).

Therefore p_{lc} remains finite in the rest frame of 'b'(L-frame) as $s \dashrightarrow \infty$ for $-1 \leqslant x < \emptyset$. Thus the region of x is defined by $-1 \leqslant x < \emptyset$ corresponds to the kinematic region where the hypothesis of limiting fragmentation is valid for breakup of the target (b).

In the rest frame of the projectile (a) for the particles with $\emptyset < x \leqslant +1$ we obtain,

$$p_{lc} = (p_t^2 + m_c^2 - x^2 m_a)/2m_a|x|, \qquad \ldots(2.38)$$

as $s \dashrightarrow \infty$.

Thus the region $\emptyset < x \leqslant +1$ corresponds to the kinematic region where the hypothesis of limiting fragmentation is valid for breakup of the projectile (a).

7. Analysis of the accelerator data showing the status of the scaling model :

An analysis of the accelerator data up to $\sqrt{s}$=53 GeV [shown in figures (2.1) to (2.5)] for p-p inclusive reactions at ISR, CERN (Capiluppi et al.,1974a,1974b) leads to the conclusion that,

(i) For pions the limiting value of the inclusive cross section is reached at small p_t for $x<\emptyset.1$ and at intermediate p_t for $x>\emptyset.1$. The approach to scaling is quicker for positive pions than their negative counterparts.

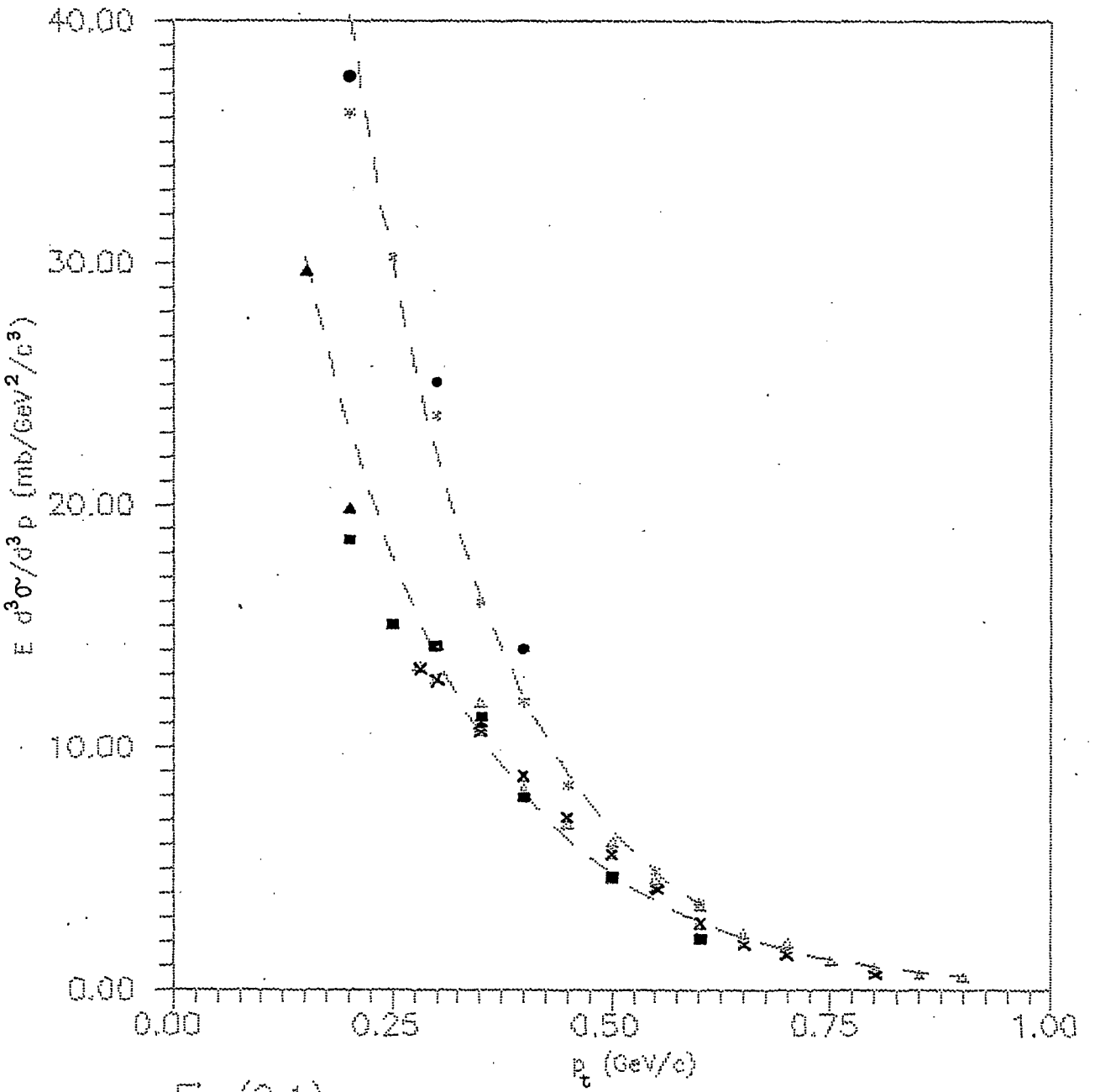
40.00
30.00
20.00
10.00
0.00
0.00
0.25
0.50
0.75
1.00
E d³σ/d³p (mb/GeV²/c³)
p_t (GeV/c)

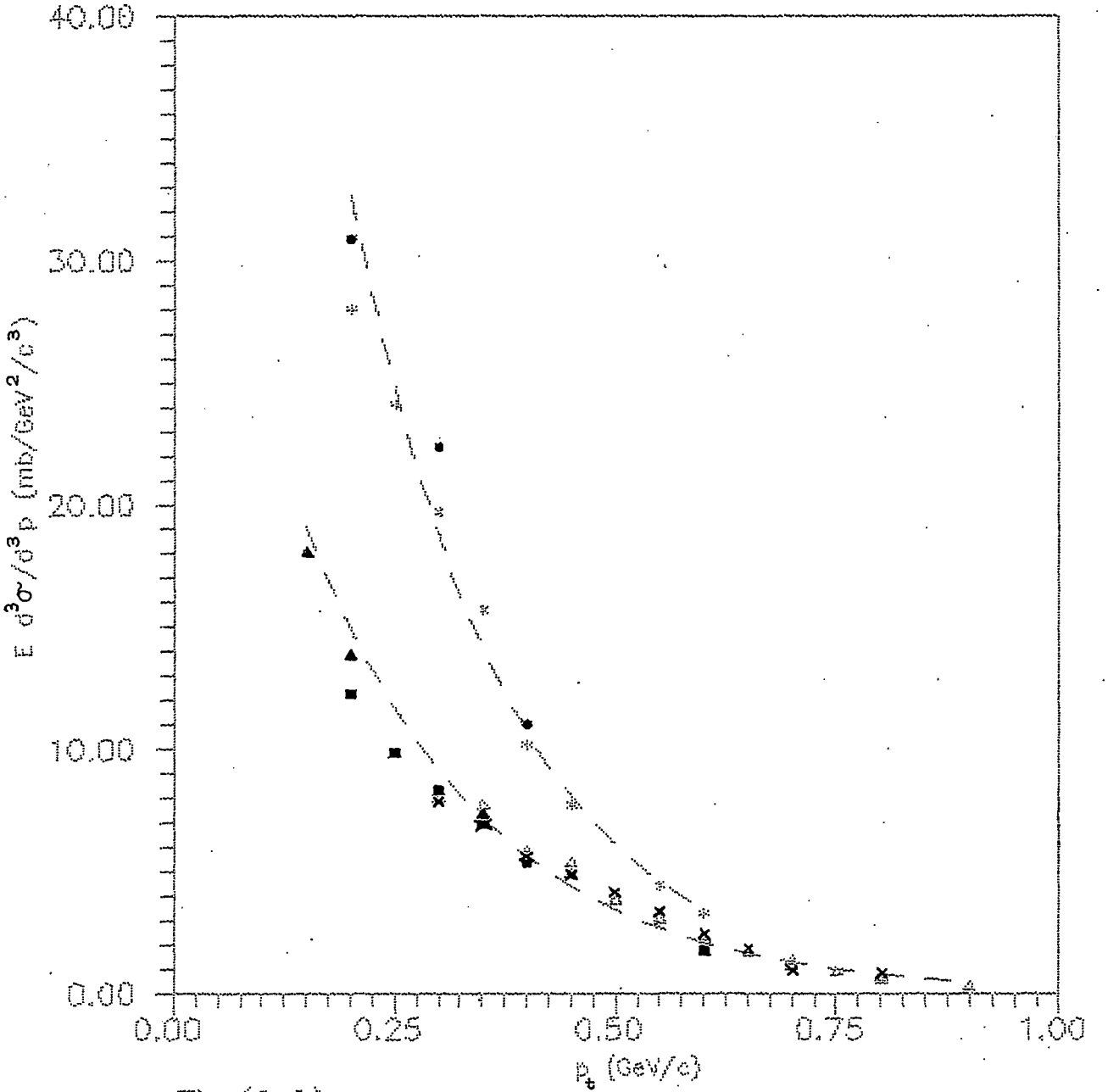
40.00
30.00
20.00
10.00
0.00
0.00
0.25
0.50
0.75
1.00
E d³σ/d³p (mb/GeV²/c³)
p_t (GeV/c)

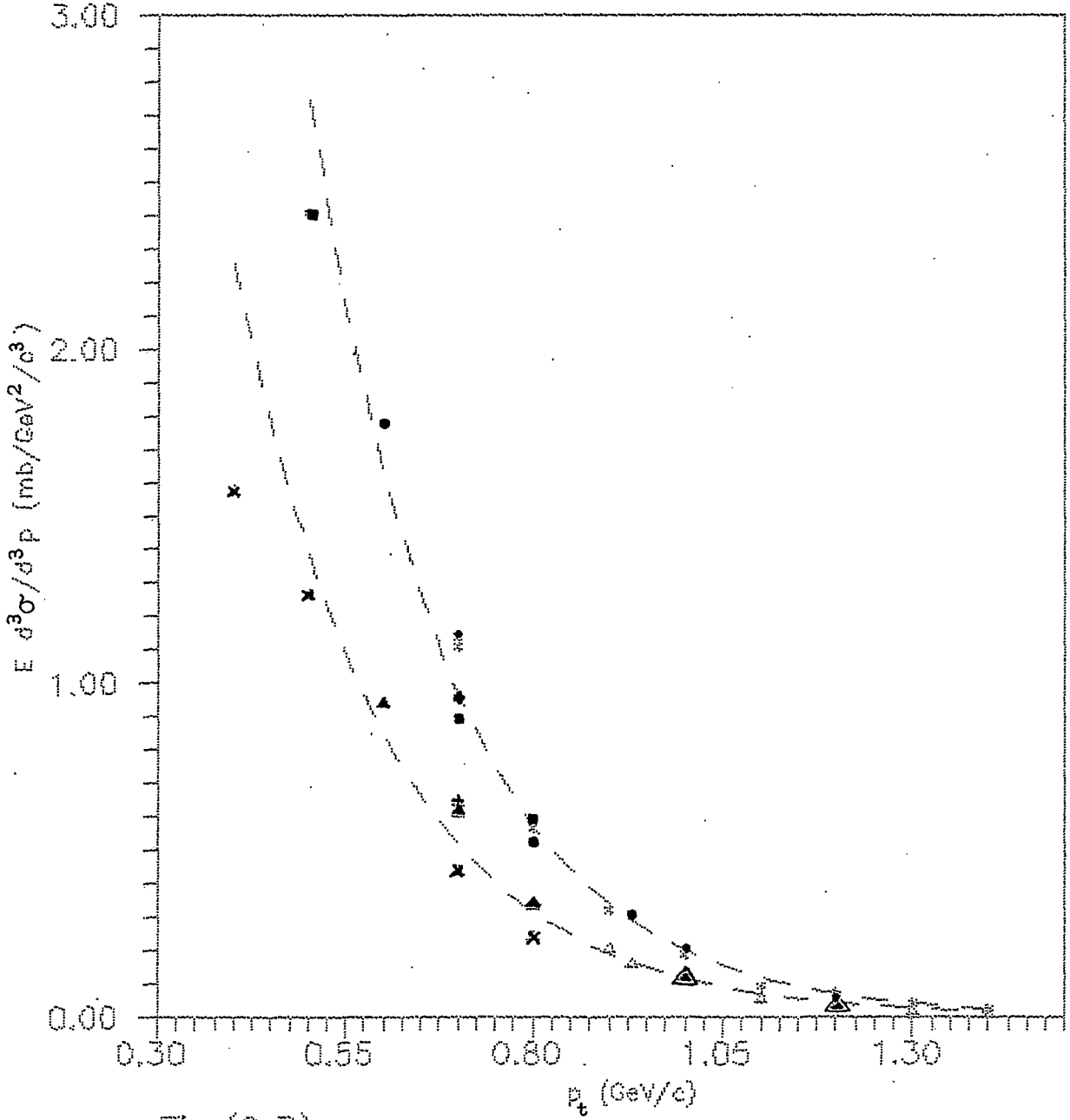
3.00
2.00
1.00
0.00
0.30
0.55
0.80
1.05
1.30
E d³σ/d³p (mb/GeV²/c³)
p_t (GeV/c)

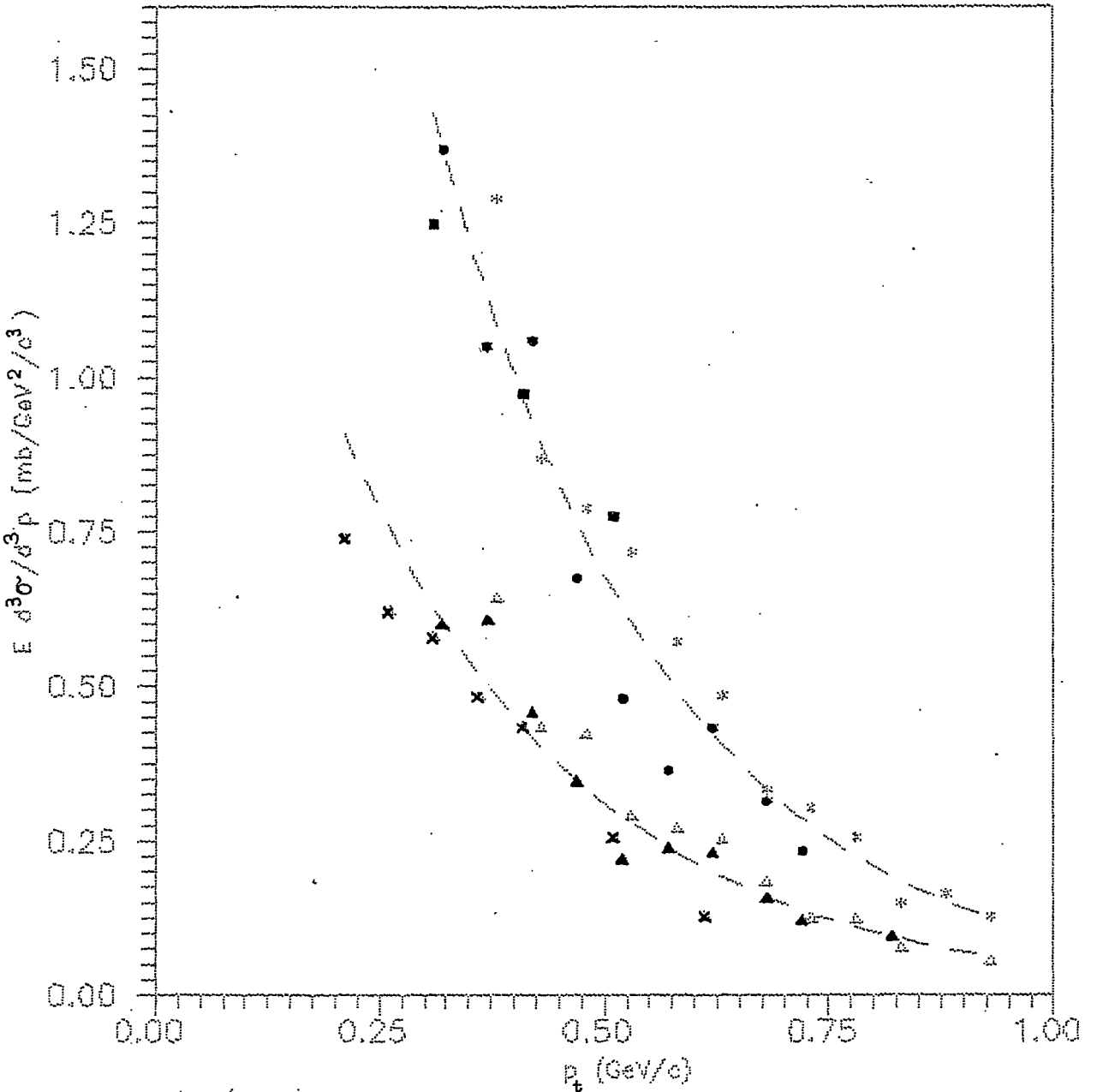
1.50
1.25
1.00
0.75
0.50
0.25
0.00
0.00
0.25
0.50
0.75
1.00
E d³σ/d³p (mb/GeV²/c³)
p_t (GeV/c)

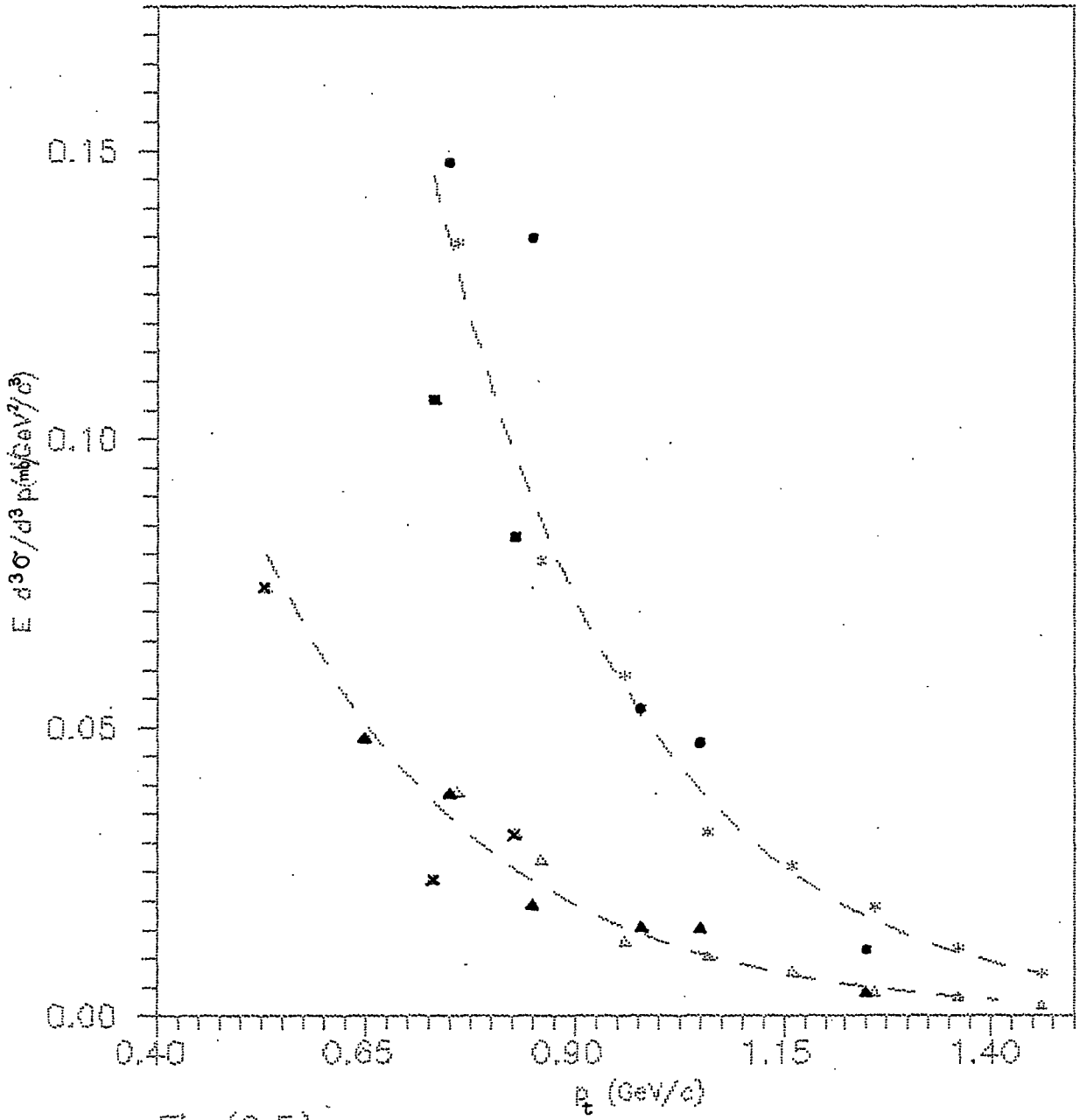
0.15
0.10
0.05
0.00
0.40
0.65
0.90
1.15
1.40
E d³σ/d³p (mb/GeV²/c³)
p_t (GeV/c)

(ii) For kaons the scaling effect is evident at intermediate p_t-values in the energy range $30.6 \leqslant \sqrt{s} \leqslant 53.0$ GeV. Scaling is reached at higher CM-energies for negative kaons in the same energy range.

In ISR experiment the variable laboratory rapidity (y_{lab}) is defined by

$$y_{lab}=y_{beam}-y = y_{beam}- \ln\{(E+p_l)/(E-p_l)\}^{1/2}, \qquad ...(2.39)$$

where y is the CM-rapidity of the produced particles and y_{beam} is the CM-rapidity of the incoming proton. In figures (2.6) to (2.9) the dependence of the invariant cross sections for p-p inclusive reactions at ISR energies on the CM-transverse momenta(p_t) at fixed values of y_{lab} are shown. The results show that,

(iii) In fragmentation region (i.e., $y_{lab}<2$) the inclusive cross sections for pions and kaons are purely exponential in p_t in the range 0.2-1.25 GeV/c at constant y_{lab} values.

(iv) The approach to scaling region are different for particles differing in mass and charge.

The results of fitting the invariant inclusive cross sections ($f=E\, d^3\sigma/d^3p$) to the expressions $f=K_1 \exp(-ap_t)$ and $f=K_2 \exp(-bp_t)$ are presented in table (2.1) for x=constant and in table (2.2) for y_{lab}=constant. From the tables one can conclude that,

(v) The shapes of the p_t distributions for pions are purely exponential for any value of y_{lab} while there are some deviations from exponential behaviour for relatively large values of x (fragmentation region).

(vi) The slopes for kaons are smaller than those for pions.

(vii) The slopes for positive pions are a little smaller than

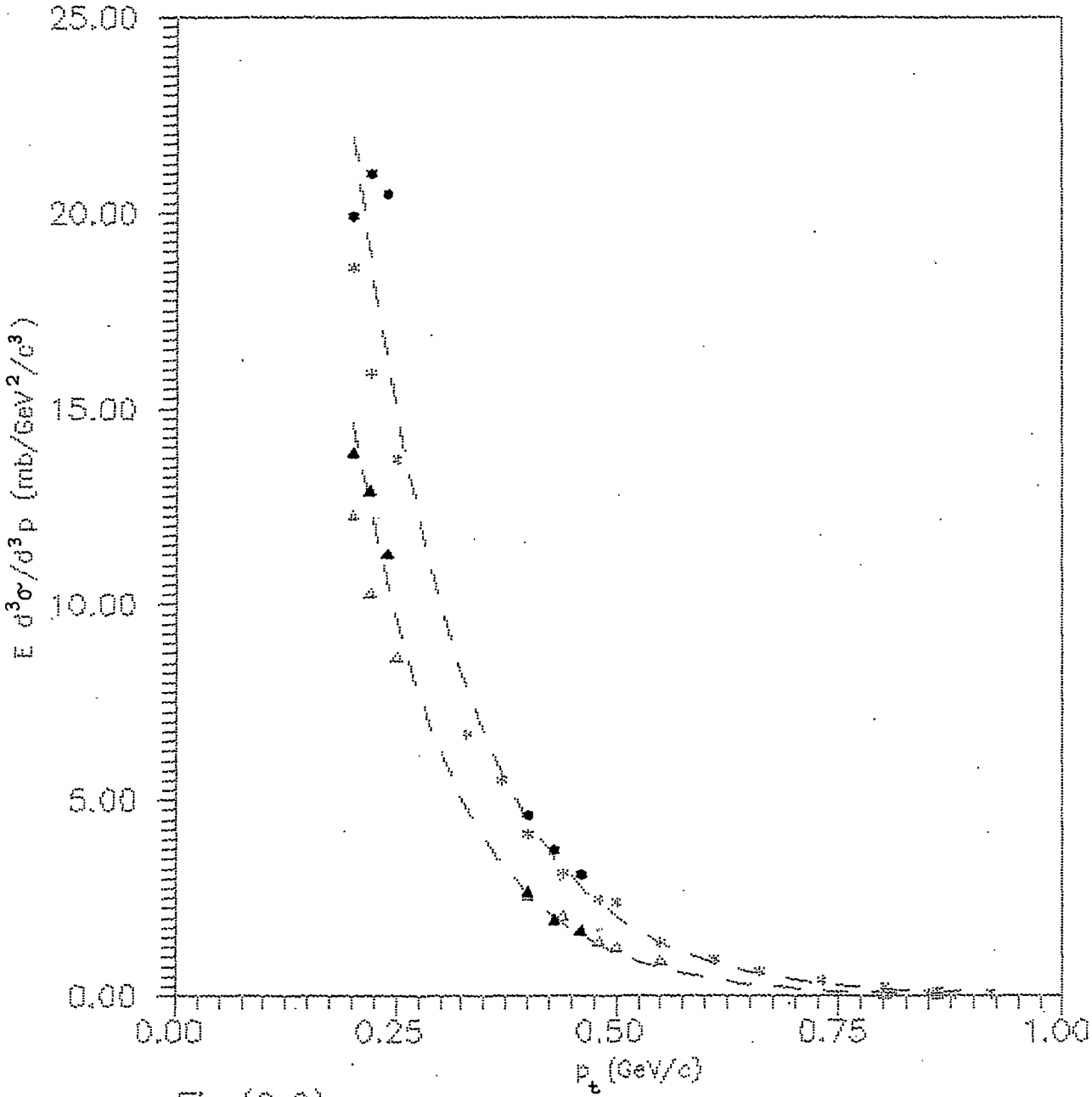
25.00
20.00
15.00
10.00
5.00
0.00
0.00
0.25
0.50
0.75
1.00
E d³σ/d³p (mb/GeV²/c³)
p_t (GeV/c)

E d³σ/dp³ (mb/GeV²/c³)
40.00
30.00
20.00
10.00
0.00
0.15
0.40
0.65
0.90
1.15
p_t (GeV/c)

E d³σ/d³p [mb/GeV²/c³)
3.50
3.00
2.50
2.00
1.50
1.00
0.50
0.00
0.15
0.40
0.65
0.90
1.15
1.40
p+ (GeV/c)

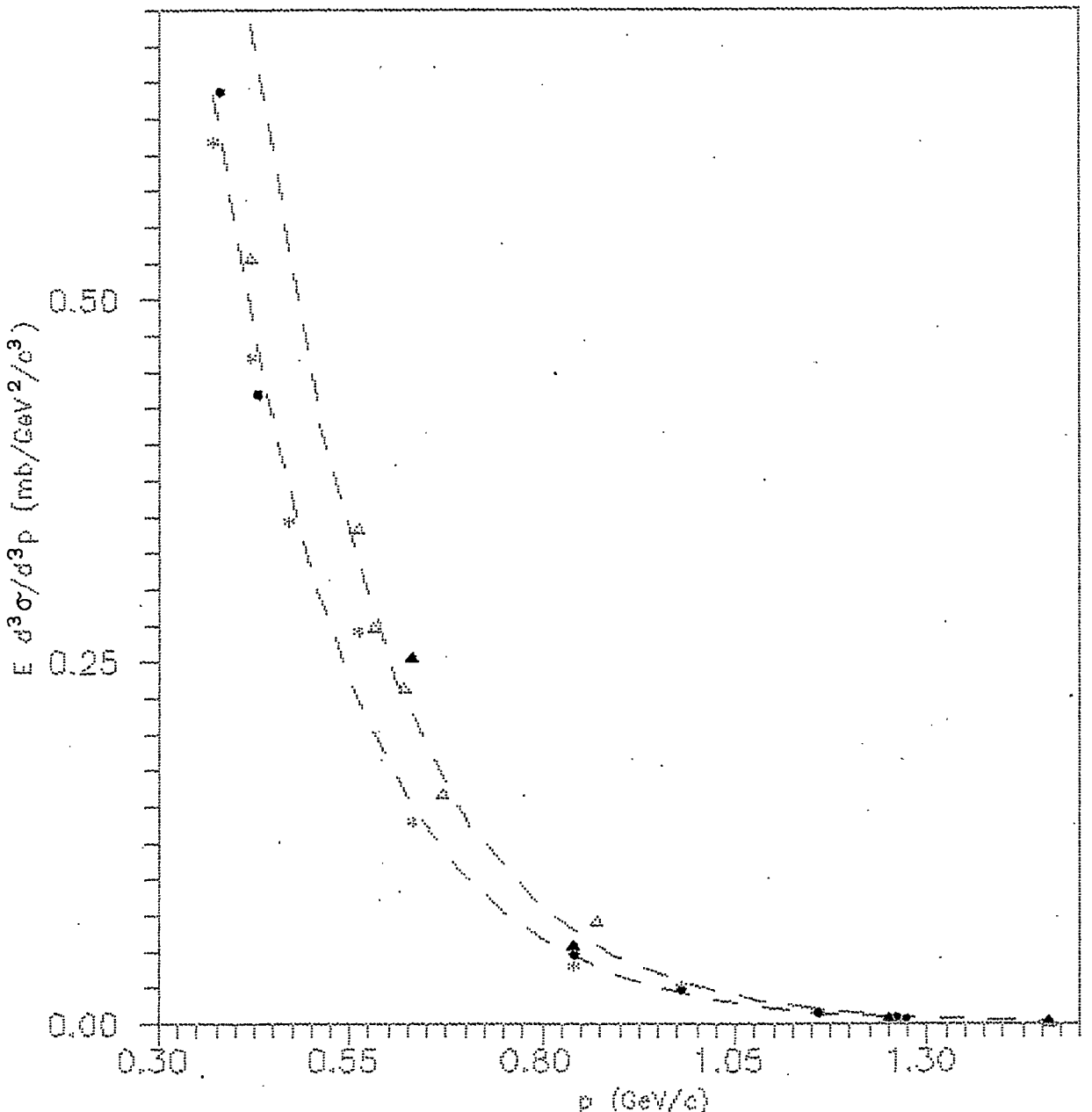
E d³σ/d³p (mb/GeV²/c³)
0.50
0.25
0.00
0.30
0.55
0.80
1.05
1.30
p (GeV/c)

those for negative pions.

(viii) The k^+ slopes are smaller than k^- ones.

(ix) The p_t dependence of the measured invariant cross section for inclusive production of neutral pions at CERN $p-\bar{p}$ collider ($\sqrt{s}$ = 540 GeV) by UA2 Collaboration (Banner et al.,1982) is shown in fig.(2.10). The results are compared to those obtained at $\sqrt{s}$ =52.7 GeV for p-p collisions (Clark et al.,1978) by an extrapolation to $\sqrt{s}$ =540 GeV. This extrapolation results in an underestimation of the cross sections in the measured p_t range ($1.5<p_t<4.5$ GeV/c).

Table 2.1 : Results of fitting the invariant inclusive cross sections ($f= E\, d^3\sigma/d^3p$) to the expression $f=K_1 \exp(-ap_t)$ for x=constant [DOF stands for degrees of freedom].

Particle	$\sqrt{s}$ -range (Gev)	x	p_t-range (GeV/c)	a $[(Gev/c)^{-1}]$	χ^2/DOF
π^+	44.6-53.0	0.075	0.2-0.6	6.013	0.571
π^-	44.6-53.0	0.075	0.2-0.6	5.597	0.830
π^+	23.3-53.0	0.15	0.15-0.9	5.246	1.659
π^-	23.3-53.0	0.15	0.15-0.9	4.889	2.226
π^+	23.3-53.0	0.30	0.5-1.4	5.223	0.765
π^-	23.3-53.0	0.30	0.4-1.4	4.922	3.087
k^+	30.6-53.0	0.16	0.31-0.93	3.931	1.041
k^-	30.6-53.0	0.16	0.21-0.93	3.695	1.332
k^+	30.6-53.0	0.32	0.73-1.46	4.103	1.200
k^-	30.6-53.0	0.32	0.53-1.46	3.846	1.216

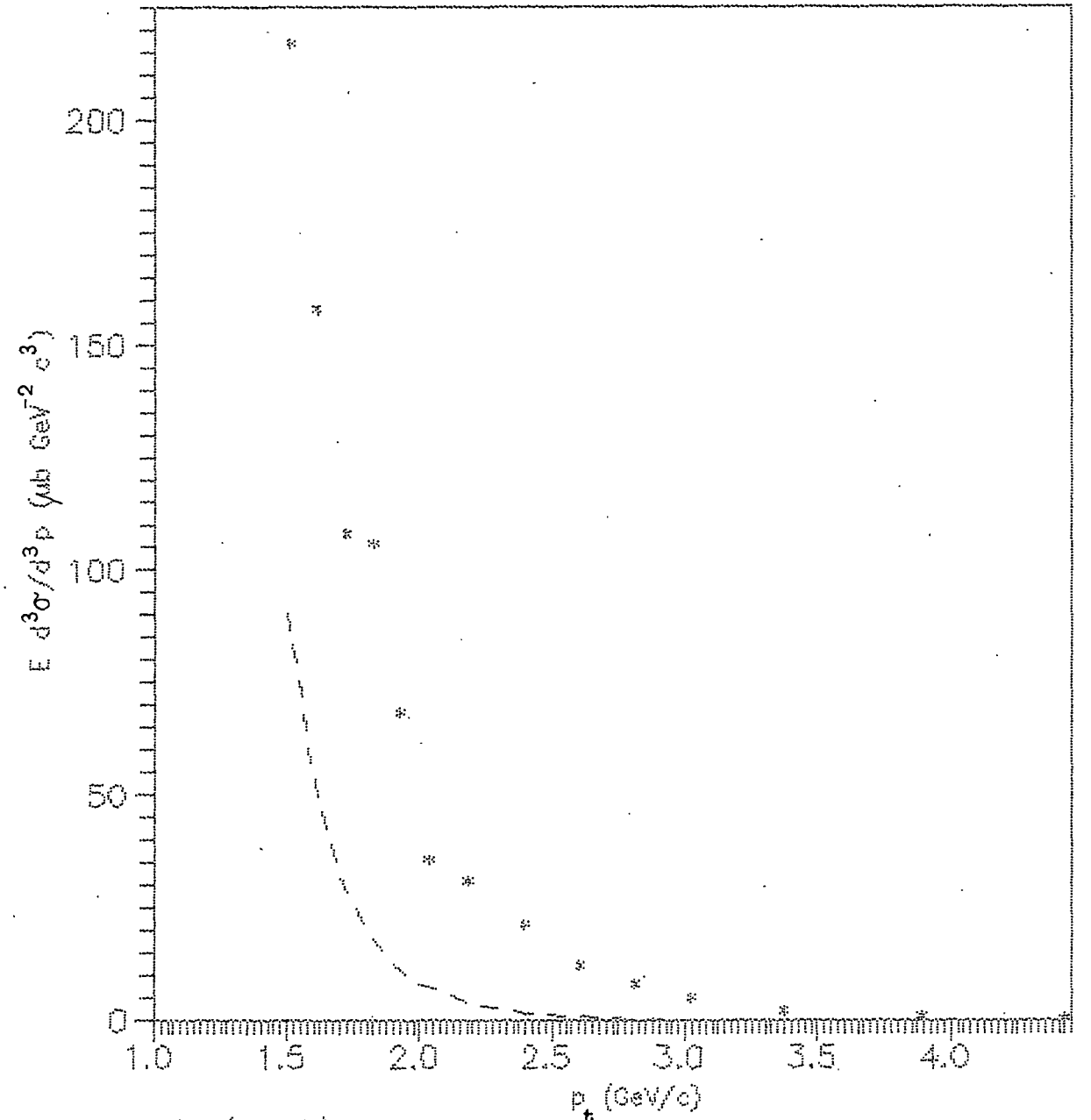
200
150
100
50
0
1.0
1.5
2.0
2.5
3.0
3.5
4.0
E d³σ/d³p (μb GeV⁻² c³)
p_t (GeV/c)

Table 2.2 : Results of fitting the invariant inclusive cross sections ($f=E\, d^3\sigma/d^3p$) to the expression $f=K_2 \exp(-bp_t)$ for y_{lab}=constant.

Particle	$\sqrt{s}$ -range (GeV)	y_{lab}	p_t-range (GeV/c)	b $[(GeV/c)^{-1}]$	χ^2/DOF
π^+	23.3-30.6	0.54	0.2-0.92	7.929	1.671
π^-	23.3-30.6	0.55	0.2-0.86	8.656	2.200
π^-	30.6-53.0	0.95	0.2-0.97	7.307	1.080
π^-	44.6-53.0	1.24	0.2-1.17	6.929	1.171
π^-	44.6-53.0	1.66	0.2-1.32	6.696	1.528
k^+	30.4-53.0	1.44	0.21-1.27	4.791	1.125
k^+	44.6-53.0	1.64	0.21-1.46	4.907	0.879
k^-	44.6-53.0	1.45	0.37-1.27	5.585	0.354
k^-	44.6-53.0	1.64	0.42-1.46	5.677	1.395

8. KNO Scaling :

Assuming that the multiparticle production cross sections obey the Feynman scaling law Koba, Nielsen and Olesen (1972) suggested another scaling law (KNO -scaling) of multiplicity distribution in hadron collisions at very high energies. The KNO prediction at sufficiently high energies has the form

$$\langle n \rangle \left[\sigma_n(s) / \sigma_{inel}^{T}(s) \right] = \psi(z), \qquad \ldots(2.40)$$

where $\sigma_n(s)$ is the partial cross section for producing a state of multiplicity n, $\sigma_{inel}^{T}(s)$ is the total inelastic cross section and $\psi(z)$, where $z=n/\langle n \rangle$; is an energy independent function. Such a scaling law leads directly to the requirement that $\langle n \rangle/D$ be a constant, where $D=(\langle n^2 \rangle - \langle n \rangle^2)^{1/2}$ is

the dispersion of the multiplicity distribution.

Dao et al (1973) found that for incident momenta greater than 50 GeV/c the quantity $\langle n \rangle / D$ appeared consistent with a constant value of $\langle n \rangle / D \simeq 2$ for A + proton collisions, where A is any one of p, $\bar{p}$, $\pi^{\pm}$, $k^{\pm}$ or γ . The energy dependence of the approach to this value varies with the type of particle A.

KNO scaling had been studied on p-p collision data in the incident momentum range 50-303 GeV/c (Slattery, 1973). Fig.(2.11) is a plot of $\langle n \rangle \sigma_n(s) / \sigma^T_{inel}(s)$ versus $z=n/\langle n \rangle$ for different incident momenta in the range 50-303 GeV/c. All the data can be expressed by an energy independent function

$$\psi(z)=(3.79z+33.7z^3-6.64z^5+0.332z^7)\exp(-3.04z), \quad ...(2.41)$$

with an overall χ^2/degree of freedom $\simeq 1$ between the function and the experimental data.

The UA5 Collaboration (Alner et al., 1984) showed clear evidence of KNO scaling violation. At $Sp\bar{p}S$ energy ($\sqrt{s}$ =540 GeV) a clear change in the shape of the scaled multiplicity distribution characterized by an enhanced probability [$P_n(s) = \sigma_n(s) / \sigma^T_{inel}(s)$] for producing high multiplicity events [$n/\langle n \rangle > 2$]. The multiplicity distribution is well described by the negative binomial distribution [fig.(2.12)],

$$P_n = C_w^{n+w-1} [(\langle n \rangle / w)/(1+\langle n \rangle / w)]^n (1+\langle n \rangle / w)^{-w}, \quad ...(2.42)$$

where the parameters $\langle n \rangle$ and w are functions of energy :

$$w = (\alpha + \beta \ln s)^{-1}, \quad ...(2.43)$$

where $\alpha = -0.098 \pm 0.008$ and $\beta = 0.0282 \pm 0.0009$ with s in GeV^2. The average multiplicity, $\langle n \rangle$ is usually parametrized as,

$$\langle n \rangle = a + b \ln s + \ln^2 s , \quad [s \text{ in } GeV^2] \quad ...(2.44)$$

with $a = 1.97 \pm 0.96$, $b = 0.21 \pm 0.29$ and $c = 0.148 \pm 0.022$.

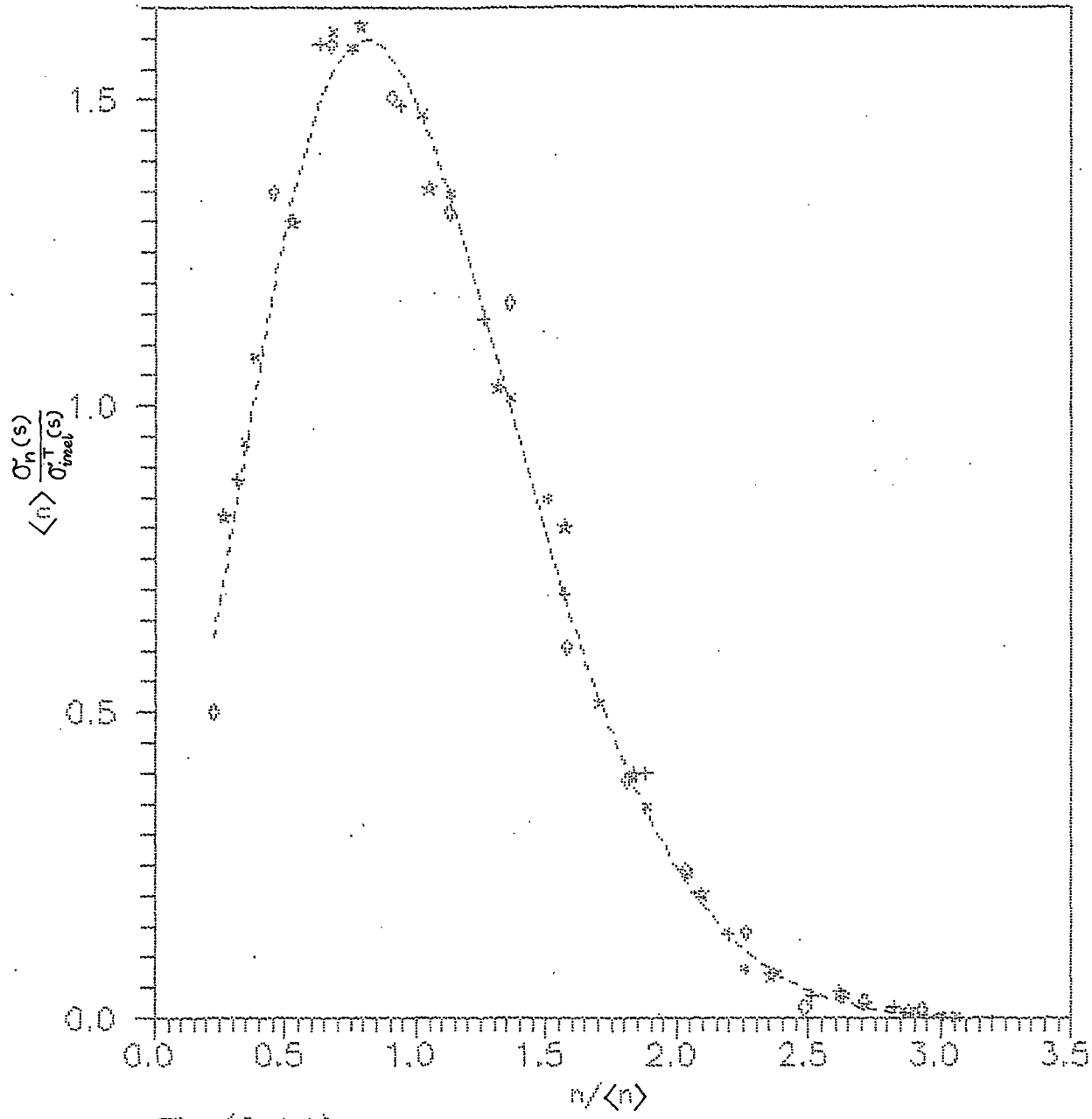
$\langle n \rangle \frac{\sigma_n(s)}{\sigma_{inel}^T(s)}$
1.5
1.0
0.5
0.0
0.0
0.5
1.0
1.5
2.0
2.5
3.0
3.5
$n/\langle n \rangle$

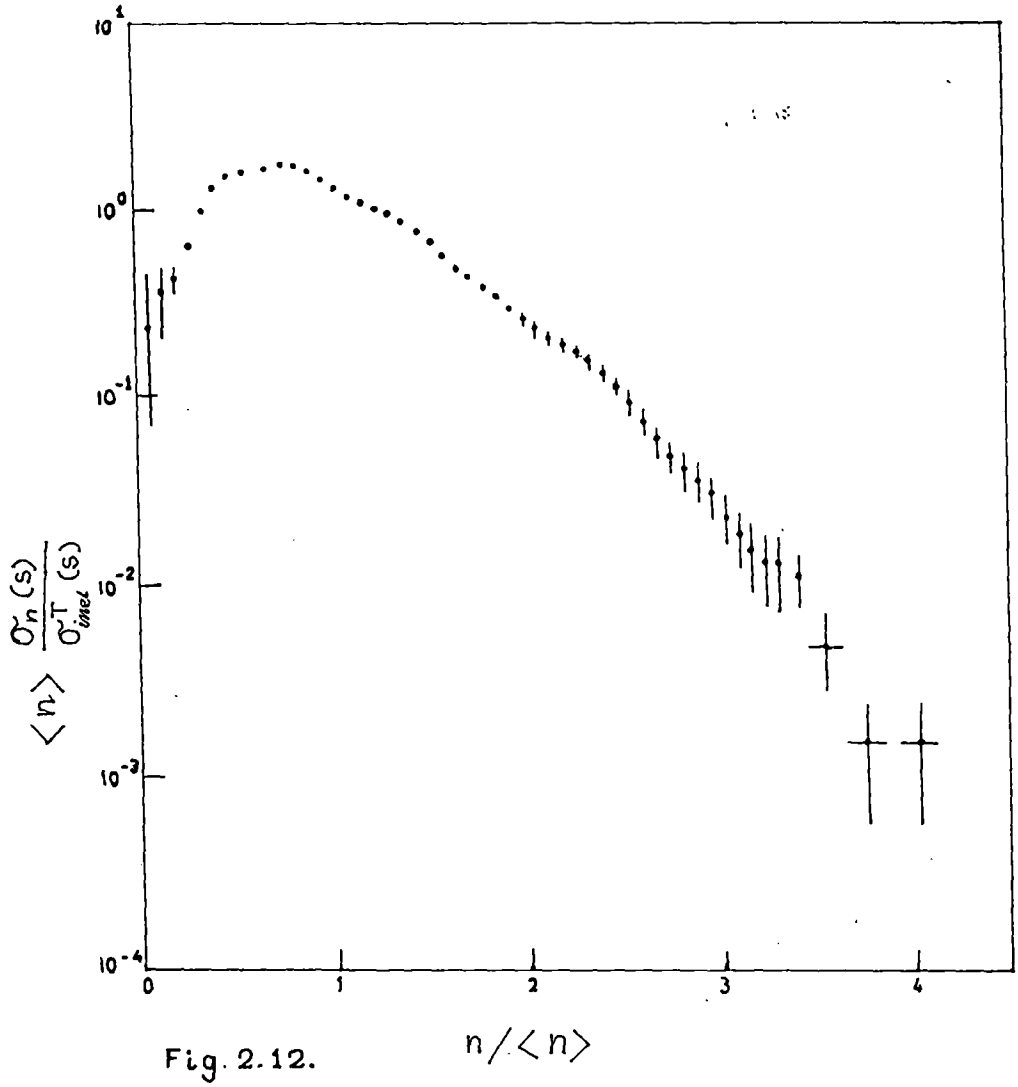
10^{1}
10^{0}
10^{-1}
10^{-2}
10^{-3}
10^{-4}
0
1
2
3
4
$\langle n \rangle \frac{\sigma_n(s)}{\sigma_{inel}^T(s)}$
$n/\langle n \rangle$

Fig. 2.12.

9. Simulation of Air Showers :

We have discussed the mechanism of the development of extensive air showers in chapter I (fig.1.1). In the earth's atmosphere an EAS develops when a high energy primary cosmic ray particle is incident on the top of the atmosphere and interacts strongly with an air nucleus depending on the interaction mean free path (L). This first interaction produces various types of mesons and baryons which further interact with the air nuclei. The interaction mean free path is given by,

$$L = A/\sigma_{inel}, \qquad \ldots(2.45)$$

where $A=2.41\times10^{4}$ if the inelastic cross section σ_{inel} is expressed in mb, then L is in gm./cm.^{2}.

One can assume that the projectile (proton, pion etc.) interacts only with a single nucleon in the air nucleus. As a consequence, the particle production cross sections in proton-air and meson-air collisions are approximated by p-p and meson-p collision results obtained (Nam et al.,1983; Giffon and Predazzi, 1984) from accelerator experiments.

The inelastic cross sections (in mb) for p-air, π-air and k-air interactions are (the incident energy, E_o in GeV):

$$\sigma_{p\text{-}air}^{inel} = 270 \text{ for } E_o<100$$
$$= 240.34+0.9638\ln E_o+0.99466\ln^2 E_o \text{ for } E_o \geq 100 \qquad \ldots(2.46)$$

$$\sigma_{\pi\text{-}air}^{inel} = 0.763\ \sigma_{p\text{-}air}^{inel} \qquad \ldots(2.47)$$

$$\sigma_{k\text{-}air}^{inel} = 175 \text{ for } E_o<100$$
$$= 71.4+14.81\ln E_o+250.7E_o^{-0.457} \text{ for } E_o \geq 100 \qquad \ldots(2.48)$$

The differential cross section for inclusive production of particles, if taken as energy independent up to certain energy, can be factorized in terms of (x, p_t) or (y, p_t) as,

$$d^2\sigma/dx\, dp_t^2 = F(x)\, G(p_t) \qquad \ldots(2.49)$$

$$d^2\sigma/dy\, dp_t^2 = f(y)\, g(p_t) \qquad \ldots(2.50)$$

The available data given by Capiluppi et al. (1974a,b) up to $\sqrt{s}$ =62.7 GeV have been fitted by the author and the functional forms obtained are the following:

$$F(x) = A(1-x)^a \qquad \ldots(2.51)$$

$$G(p_t) = B \exp(-bp_t) \qquad \ldots(2.52)$$

$$f(y) = C \exp(\alpha y) \qquad \ldots(2.53)$$

$$g(p_t) = D \exp(-\beta p_t) \qquad \ldots(2.54)$$

The values of the two sets of constants, (A,B,a,b) and (C,D,α,β) for various particles are given in tables (2.3) and (2.4) respectively:

Table 2.3:Values of the constants in the functions F(x) and G(p_t)

Particle	A	a	B	b[(GeV/c)$^{-1}$]
π^+	22.60	4.644	79.19	5.494
π^-	19.11	5.555	51.93	5.136
k^+	2.10	3.886	3.87	4.017
k^-	1.42	6.282	1.29	3.770

Table 2.4:Values of the constants in the functions f(y) and g(p_t)

Particle	C	α	D	β[(GeV/c)$^{-1}$]
π^+	3.54	1.196	107.22	7.929
π^-	2.30	1.193	116.64	7.397
k^+	0.18	1.398	7.77	4.849
k^-	0.05	2.142	6.28	5.631

The dependence of average inelasticities with incident energy (E_o in GeV) for various types of particles (Antonov et al.,1983) are :

$\langle K_{p-air}\rangle = 0.55$, for $E_o < 100$

$= 0.55 + [\{0.02 \ln(E_o/100)\}/\{1+0.04\ln(E_o/100)\}]$, for $E_o \geq 100$ ...(2.55)

$\langle K_{\pi-air}\rangle = 0.70$, for $E_o < 100$

$= 0.70 + [\{0.02 \ln(E_o/100)\}/\{1+0.04\ln(E_o/100)\}]$, for $E_o \geq 100$ ...(2.56)

$\langle K_{k-air}\rangle = \langle K_{\pi-air}\rangle$ ...(2.57)

The energy dependence of the transverse momenta (p_t in GeV/c) of the produced secondaries are different for different kinds of secondaries produced :

$$\langle p_t\rangle_p = 0.0471+0.0059 \ln(E_o/100) \quad ...(2.58)$$

$$\langle p_t\rangle_\pi = 0.326+0.0075 \ln(E_o/100) \quad ...(2.59)$$

$$\langle p_t\rangle_k = 0.423+0.0052 \ln(E_o/100) \quad ...(2.60)$$

The multiplicity distribution of the produced secondaries may be taken as negative binomial distribution (Alner et al.,1985) of the form :

$$P_n = C_w^{n+w-1}[(\langle n\rangle/w)/(1+\langle n\rangle/w)]^n (1+\langle n\rangle/w)^{-w}, \quad ...(2.61)$$

where $w = (-0.098+0.0282 \ln s)^{-1}$, ...(2.62)

s is the CM-energy squared in GeV^2.

The dependence of the average multiplicity, $\langle n\rangle$ on CM-energy is parametrized as,

$$\langle n\rangle = 1.97+0.21 \ln s+0.148 \ln^2 s \quad ...(2.63)$$

$$\text{Or, } \langle n\rangle = -7.4+7.6\, s^{0.124}, \quad ...(2.64)$$

with s in GeV^2.

For interpretation of experimental EAS data above results from

accelerator experiments available so far are to be used for simulation of EAS with a computer. Computer simulations of EAS provide a connection between experimental air shower data and high energy interaction model as well as primary cosmic ray mass composition model. The principle of EAS simulation is indicated below :

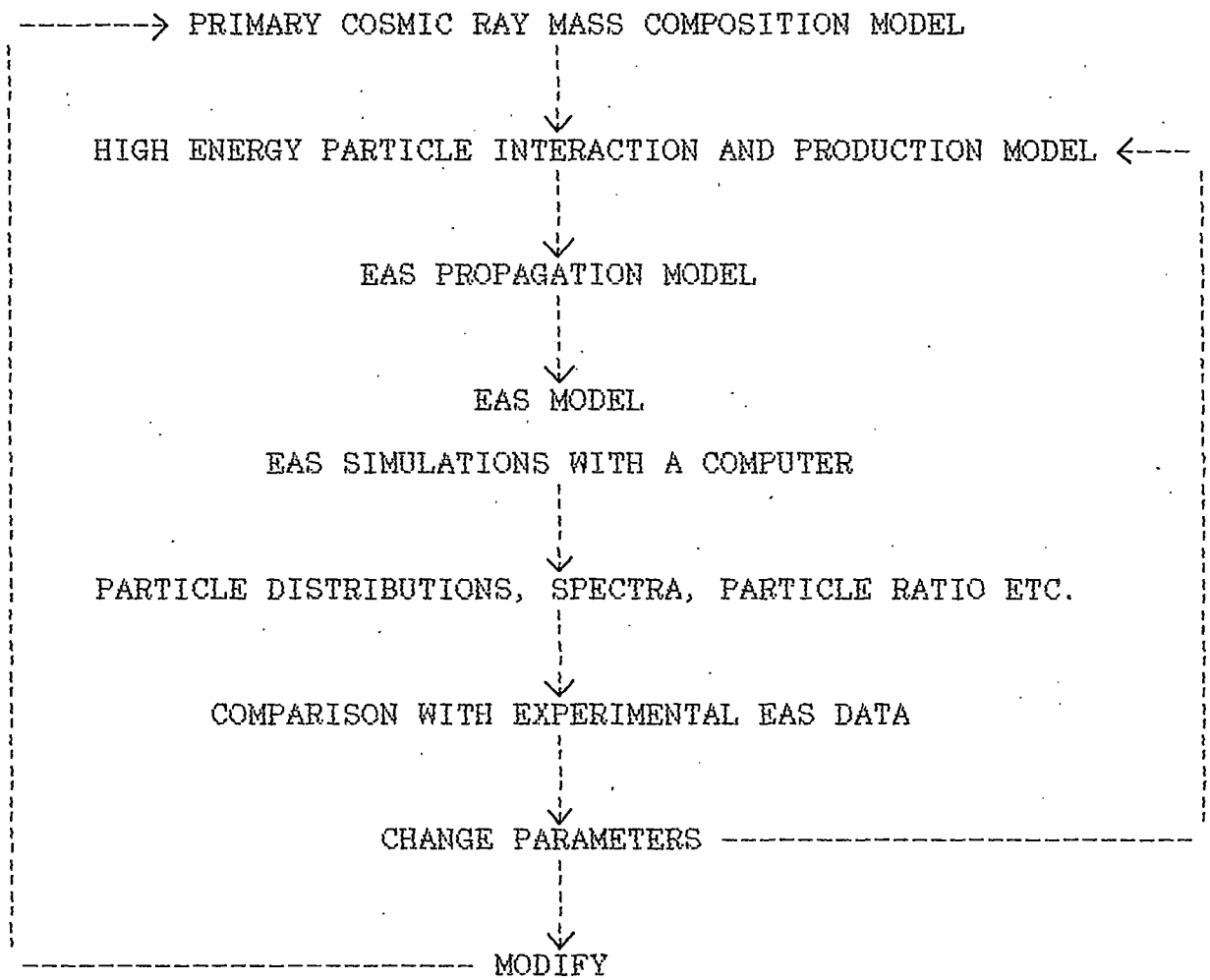

In Monte Carlo simulation of air showers widely varying primary mass composition have been used (Wrotniak and Yodh,1985a,b,c; Procureur et al.,1988; Dai et al.,1988; Capdevielle et al.,1988; Bourdeau et al.,1988; Szabelski et al.,1989; Capdevielle and Gabinski,1990; Trzupek et al.,1992). By changing the nuclear interaction parameters and the mass of the primary particle

various air shower models have been proposed. By comparing the air shower observables with those obtained from model calculations it is possible to test the sensitivity of various high energy nuclear interaction models.

Some basic features of four interaction models chosen by Wrotniak and Yodh (1985) are given below :

Model F-YØØ :

Primary particle : Proton

Mean free path for inelastic interaction : Energy independent, 75 gm./cm**2 for nucleons, 11Ø gm./cm**2 for pions and 13Ø gm./cm**2 for kaons.

Inelasticity : Uniform in (Ø,1) for nucleons and (1/3,1) for mesons.

Inclusive distribution in x for secondaries : Energy independent, obtained by scaling extrapolation of the ISR data.

Secondaries produced : 6Ø% charged pions, 3Ø% neutral pions, 5% charged kaons and 5% neutral kaons.

Model M-FØØ :

Primary particle : Proton

Mean free path for inelastic interaction :
Below 1 TeV : 84 gm./cm**2 for nucleons and 117 gm./cm**2 for pions and kaons.
Above 1 TeV : $L(E_o)=L_o/(1+Ø.ØØ383\ln E_o)$

Inelasticity : Same as F-YØØ

Inclusive distribution in x for secondaries :
Below 1 TeV: same as F-YØØ.
Above 1 TeV: the functional shape is unchanged but the scale x-value decreases as 1/(s**Ø.Ø625).

Secondaries produced : Below 1 TeV: same as F-YØØ.
Above 1 TeV: the fractions of kaons and neutral pions increase with energy, reaching 6.8% (each) and 53.7%, respectively at 1 EeV.

Model FF-YØØ :

Primary particle : Heavy nuclei (alpha particle to iron).

Mean free path for inelastic interaction : Energy independent - ranging from 37 gm./cm**2 for alpha particles to 16 gm./cm**2 for iron.

The other basic features are the same as F-YØØ.

Model RM-FØØ :

Primary particle : Heavy nuclei (alpha particle to iron).

Mean free path for inelastic interaction : The effect of rise in cross section with increase in energy which results in decrease in mean free path is included. For iron group the mean free paths decrease from 12.2 to 1Ø.6 gm./cm**2 between 1ØØ TeV and 1 EeV.

The other basic features remain the same as M-FØØ.

Figure captions :

Fig.(2.1) : The invariant inclusive cross sections ($Ed^3\sigma/d^3p$) for the production of π^+versus transverse momentum (p_t) for x=Ø.15 at CM energies : ▲ 23.3 GeV, ■ 3Ø.6 GeV, x 44.6 GeV, Δ 53.Ø GeV and for x=Ø.Ø75 at CM energies : ● 44.6 GeV, * 53.Ø GeV. The dashed lines represent interpolations of the data by the author.

Fig.(2.2) : $Ed^3\sigma/d^3p$ vs. p_t for the inclusive production of $\pi^-$for x=Ø.15 at CM energies : ▲ 23.3 GeV, ■ 3Ø.6 GeV, x 44.6 GeV, Δ 53.Ø GeV and for x=Ø.Ø75 at CM energies : ● 44.6 GeV, * 53.Ø GeV. The dashed lines represent interpolations of the data by the author.

Fig.(2.3) : $Ed^3\sigma/d^3p$ vs. p_t at x=Ø.3Ø for the inclusive production of π^+at CM energies : ◆ 23.3 GeV, ■ 3Ø.6 GeV, ● 44.6 GeV, * 53.Ø GeV and of π^-at CM energies :+ 23.3 GeV, x 3Ø.6 GeV, ▲ 44.6 GeV, Δ 53.Ø GeV. The dashed lines represent interpolations of the data by the author.

Fig.(2.4) : $Ed^3\sigma/d^3p$ vs. p_t at x=Ø.16 for the inclusive production of k^+ at CM energies: ■ 3Ø.6 GeV, ● 44.6 GeV, * 53.Ø GeV and of k^- at CM energies : x 3Ø.6 GeV, ▲ 44.6 GeV, Δ 53.Ø GeV. The dashed lines represent interpolations of the data by the author.

Fig.(2.5) : $Ed^3\sigma/d^3p$ vs. p_t at x=Ø.32 for the inclusive production of k^+ at CM energies: ■ 3Ø.6 GeV, ● 44.6 GeV, * 53.Ø GeV and of k^- at CM energies : x 3Ø.6 GeV, ▲ 44.6 GeV, Δ 53.Ø GeV. The dashed lines represent interpolations of the data by the author.

Fig.(2.6) : $Ed^3\sigma/d^3p$ vs. p_t at y_{lab}=Ø.54 for the inclusive production of π^+at CM energies: ● 23.3 GeV, * 3Ø.6 GeV and of π^-at y_{lab}=Ø.55 at CM energies : ▲ 23.3 GeV, Δ 3Ø.6 GeV. The dashed lines represent interpolations of the data by the author.

Fig.(2.7) : $Ed^3\sigma/d^3p$ vs. p_t for the inclusive production of π^-at

y_{lab}=Ø.95 at CM energies : ● 3Ø.6 GeV, * 44.6 GeV, x 53.Ø GeV, at y_{lab}=1.24 at CM energies : ▲ 44.6 GeV, Δ 53.Ø GeV and at y_{lab}=1.66 at CM energies : ★ 44.6 GeV, ☆ 53.Ø GeV. The dashed lines represent interpolations of the data by the author.

Fig.(2.8) : $Ed^3\sigma/d^3p$ vs. p_t for the inclusive production of k^+ at y_{lab}=1.44 at CM energies : x 3Ø.4 GeV, * 44.6 GeV, ● 53.Ø GeV and at y_{lab}=1.64 at CM energies : Δ 44.6 GeV, ▲ 53.Ø GeV. The dashed lines represent interpolations of the data by the author.

Fig.(2.9) : $Ed^3\sigma/d^3p$ vs. p_t for the inclusive production of k^- at y_{lab}=1.45 at CM energies : * 44.6 GeV, ● 53.Ø GeV and at y_{lab}=1.64 at CM energies : Δ 44.6 GeV, ▲ 53.Ø GeV. The dashed lines represent interpolations of the data by the author.

Fig.(2.1Ø) : The invariant cross sections for the inclusive production of π° at $\sqrt{s}$=54Ø GeV (*) are compared to those obtained at $\sqrt{s}$=52.7 GeV by an extrapolation to $\sqrt{s}$=54Ø GeV (----).

Fig.(2.11) : Distribution of charged particle multiplicity plotted as a function of z for different incident momenta (* 5Ø GeV/c, x 69 GeV/c, + 1Ø2 GeV/c, ☆ 2Ø5 GeV/c, ◇ 3Ø3 GeV/c). The dashed curve represent the energy independent function given by equation (2.41).

Fig.(2.12) : Charged multiplicity distribution plotted as a function of z for UA5 data.